Int. J. Heat Mass Transfer. Vol. 31, No. 9, pp. 1885–1898, 1988
Printed in Great Britain

0017–9310/88 $3.00 + 0.00

The ITPE technique applied to steady-state ground-coupling problems

MONCEF KRARTI,† DAVID E. CLARIDGE‡ and JAN F. KREIDER†

† Joint Center for Energy Management, CEAE Department, University of Colorado, Boulder, CO 80309-0428, U.S.A.
‡ Department of Mechanical Engineering, Texas A&M University, College Station, TX 77843-3123, U.S.A.

(*Received* 18 *August* 1987 *and in final form* 8 *February* 1988)

Abstract—A new analytical procedure called interzone temperature profile estimation (ITPE) is presented and applied to determine the two-dimensional steady-state temperature distribution within earth around a building. The solutions of the governing heat conduction equations are derived for two common ground-coupling geometries: slab-on-grade floors and rectangular basements. A water table at constant temperature is assumed to exist at a given depth below the soil surface. The solutions presented are the first analytic solutions for these geometries capable of considering the effects of both insulation and the presence of a water table on heat flow from these geometries.

1. INTRODUCTION

WHEN A steady-state heat conduction problem is too complicated to be solved by analytical techniques, graphical means, electrical analogies or numerical techniques are normally utilized. However, in most cases numerical techniques such as finite differencing provide numerical answers to a specific problem without much physical insight.

This paper presents a new procedure for solving a class of complicated heat conduction problems. This procedure combines numerical and analytical techniques to arrive at the functional form of heat conduction solutions that otherwise cannot be obtained by solely applying the classical analytical methods. The new procedure, called interzone temperature profile estimation (ITPE), allows an understanding of the heat flux mechanism within and at the boundaries of a conducting medium.

When first introduced in ref. [1], the ITPE technique used an approximate estimation of the temperature profiles along surfaces that divide the conducting medium into zones where the heat conduction equation can be easily solved. Two applications of the ITPE technique to ground-coupled heat transfer were treated, the insulated slab-on-grade problem in ref. [2] and the insulated full-rectangular-basement problem in ref. [3]. In this paper, the ITPE technique is improved by introducing a method that leads to a very good estimation of the temperature profiles, and consequently to more accurate solutions of the heat conduction equation.

The idea of the ITPE technique consists of assuming that the temperature variation along adequate surfaces inside the ground (or any other medium) is known. These surfaces are those imposed by either of the following cases.

(1) Geometric configuration, such as a rectangular basement shape.

(2) Boundary condition, such as an insulated slab-on-grade floor adjacent to a soil surface kept at a constant temperature.

Instead of the approximate exponential form for the temperature profile expressions used in the preliminary work [2, 3] an 'exact' form is determined by imposing heat flux continuity along the surface where one of the two cases cited above occurs. As will be shown later in this paper, these 'exact' forms are, in most cases, obtained through the use of the Gauss–Jordan elimination method.

Due to the mathematical complexity, analytical solutions for basement configurations are extremely limited. Shelton [4] determined the steady-state heat loss from a hemisphere embedded in the ground. Boileau and Latta [5] developed a steady-state solution for basements based on the *assumption* that heat flows follow circular arcs. Their solution is the basis for the method which has been provided in the *ASHRAE Handbook* [6] for over a decade for calculating maximum losses at design conditions. Other analytical solutions are those developed by Shen and Ramsey [7] and Claesson and Eftring [8]. Shen and Ramsey [7] used the least square Fourier series method to estimate heat losses from insulated underground buildings, but they did not account for water table effects. Claesson and Eftring [8] computed the steady-state optimal thermal insulation distribution for several underground configurations. However, the heat losses for insulation other than optimal are not given. Most of the analytical solutions and design methods for basement and slab-on-grade heat loss are reviewed in ref. [9].

This paper analyzes the two most common ground-coupled structures: slabs and basements. The prime

NOMENCLATURE

a	half width of ground-coupled building [m]
A_n, B_n, C_n	general term in a Fourier series expansion
b	water table depth [m]
c	basement depth [m]
f, g	functions of one of the space coordinates [K]
f_n, g_n	Fourier coefficients
H	ratio, h/k_s [m^{-1}]
h	overall heat transfer conductance [$W m^{-2} K^{-1}$]
h_i	inside surface convective heat transfer coefficient [$W m^{-2} K^{-1}$]
h_o	outside surface convective heat transfer coefficient [$W m^{-2} K^{-1}$]
k_s	soil thermal conductivity [$W m^{-1} K^{-1}$]
L	distance from building center to a boundary where soil temperature is undisturbed [m]
T	temperature [K]
T_i	building air temperature [K]
T_w	water table temperature [K]
T_0	slab temperature [K]
T_1	soil surface temperature [K]
ΔT_0	dimensionless temperature
U_o	envelope material conductance [$W m^{-2} K^{-1}$]
U_i	insulation conductance [$W m^{-2} K^{-1}$].

Greek symbols

α, β, γ	coefficients defined in equations (6) and (16)
α', β', γ'	coefficients defined in equation (18)
$\zeta_n, \chi_n, \nu_n, \mu_n$	eigenvalues [m^{-1}].

Subscripts

f	floor
wl	walls
I	zone (I)
II	zone (II)
III	zone (III).

objective of this study is to determine the effects of thermal insulation and the water table on the steady-state soil temperature distribution. Note that this analysis can be used to determine the yearly average heat losses from basements and slabs.

The second section discusses the two-dimensional steady-state heat conduction solution underneath a slab-on-grade floor. The special case of a non-insulated slab is analyzed in some detail. The effect of the depth and the temperature of a water table below the slab floor is determined and conclusions are drawn.

The temperature distribution around an insulated rectangular basement is the subject of the third section. While the insulation along the walls and the floor is assumed uniform, the insulation of the walls can be different from the insulation of the floor. The effect of a water table, at some depth below the basement floor, is also shown.

2. INSULATED SLAB-ON-GRADE FLOOR

2.1. *General solution*

Even when a slab floor is not insulated, the temperature along its width is not constant. A thermal resistance exists between room air and the slab surface. To account for this resistance, an interface conductance h is usually introduced and a third-kind boundary condition is used. This boundary condition expresses the continuity of the heat flux between the lower slab surface and the interior air (at T_i) via (1) the convective conductance h_o to the ambient air above the slab, (2) the insulation conductance U_i, (3) the slab material conductance U_s, and (4) the interface contact conductance h_i. Therefore, the boundary condition at the slab surface can be written as

$$k_s \left.\frac{\partial T}{\partial y}\right|_{y=0} = h[T(x,0) - T_i]$$

where h is the equivalent air–insulation–slab–soil conductance, given by

$$h = (h_o^{-1} + U_i^{-1} + U_s^{-1} + h_i^{-1})^{-1} \qquad (1)$$

and k_s the thermal conductivity of the soil (assumed isotropic), while T_i is the air temperature above the slab (i.e. the building interior temperature).

Consequently, the steady-state temperature distribution $T(x, y)$ inside the ground for an insulated slab-on-grade floor configuration as shown in Fig. 1 can be determined by solving the following equation:

$$\frac{\partial^2 T}{\partial x^2} + \frac{\partial^2 T}{\partial y^2} = 0 \qquad (2)$$

with

$$T = T_w \quad \text{for } y = b$$

$$T = T_1 \quad \text{for } y = 0 \text{ and } |x| > a$$

$$\frac{\partial T}{\partial y} = H(T - T_1) \quad \text{for } y = 0 \text{ and } |x| < a$$

where H is the ratio of the equivalent air–insulation–slab–soil conductance to the soil thermal conductivity (i.e. $H = h/k_s$).

The equation above cannot be solved by formal

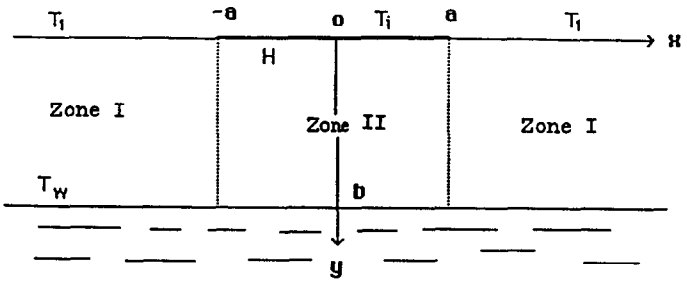

FIG. 1. Slab-on-grade floor configuration with finite water table level.

techniques such as the Schwarz–Christoffel transformation used in ref. [10]. However, the ITPE approach can be used. Figure 1 shows that the surfaces, $x = -a$ and a divide the ground medium into three zones.

Because of the symmetry around the axis $x = 0$, the temperature $T(x, y)$ will be determined only in zones (I) and (II). Let $f(y)$ be the temperature profile along the surface $x = -a$; then the solution of equation (2) in zone (I) is

$$T_{\mathrm{I}}(x,y) = \frac{2}{b}\sum_{n=1}^{\infty}\frac{\sin \nu_n y}{\nu_n} \times \{[T_{\mathrm{I}} - (-1)^n T_{\mathrm{w}}][1 - \mathrm{e}^{\nu_n(x+a)}] + \nu_n f_n \mathrm{e}^{\nu_n(x+a)}\} \quad (3)$$

while in zone (II), the temperature $T_{\mathrm{II}}(x, y)$ is given by

$$T_{\mathrm{II}}(x,y) = \frac{2}{b}\sum_{n=1}^{\infty} f_n \sin \nu_n y \frac{\cosh \nu_n x}{\cosh \nu_n a} - \frac{2}{a} T_{\mathrm{w}} \sum_{n=1}^{\infty} \frac{(-1)^n}{\mu_n} \cos \mu_n x \frac{\sinh \mu_n y}{\sinh \mu_n b} - \frac{2}{a}\sum_{n=1}^{\infty} (-1)^n C_n \cos \mu_n x \frac{\sinh \mu_n (b-y)}{\sinh \mu_n b} \quad (4)$$

where

$$\nu_n = \frac{n\pi}{b}; \quad f_n = \int_0^b f(y) \sin \nu_n y \, \mathrm{d}y; \quad \mu_n = \frac{(2n-1)\pi}{2a}$$

and

$$C_n = \frac{HT_{\mathrm{i}}/\mu_n + T_{\mathrm{w}}/\sinh \mu_n b + \frac{2}{b}\sum_{m=1}^{\infty} f_m \mu_n \nu_m/(\mu_n^2 + \nu_n^2)}{(H + \mu_n \coth \mu_n b)}.$$

The continuity of the heat flux at the surface $x = -a$, gives the condition

$$\left.\frac{\partial T_{\mathrm{I}}}{\partial x}\right|_{x=-a} = \left.\frac{\partial T_{\mathrm{II}}}{\partial x}\right|_{x=-a} \quad (5)$$

or

$$\frac{2}{b}\sum_{n=1}^{\infty} \sin \nu_n y \{\nu_n f_n - [T_{\mathrm{I}} - (-1)^n T_{\mathrm{w}}]\} = \frac{-2}{b}\sum_{n=1}^{\infty} \nu_n \tanh \nu_n a \, f_n \sin \nu_n y + \frac{2}{a} T_{\mathrm{w}} \sum_{n=1}^{\infty} \frac{\sinh \mu_n y}{\sinh \mu_n b} + \frac{2}{a}\sum_{n=1}^{\infty} \mu_n C_n \frac{\sinh \mu_n (b-y)}{\sinh \mu_n b}.$$

The Fourier coefficients f_n are obtained through use of the Fourier inverse integrals by multiplying the above equality by $\sin \nu_p y$ $(p = 1, 2, \ldots)$, and integrating the resultant equation over $[0, b]$ which yields

$$\nu_p f_p - [T_{\mathrm{I}} - (-1)^p T_{\mathrm{w}}] = -\nu_p f_p \tanh \nu_p a - (-1)^p T_{\mathrm{w}} \tanh \nu_p a + \frac{2}{a}\sum_{n=1}^{\infty} C_n \frac{\nu_p \mu_n}{\mu_n^2 + \nu_p^2}.$$

After rearrangement, this expression can be put in the form

$$f_p = \alpha_p + \sum_{m=1}^{\infty} \beta_{m,p} f_m \quad (6)$$

where

$$\alpha_p = \frac{1}{\nu_p(1 + \tanh \nu_p a)} \left\{[T_{\mathrm{I}} - (-1)^p T_{\mathrm{w}}] - (-1)^p T_{\mathrm{w}} \tanh \nu_p a + \frac{2}{a}\sum_{n=1}^{\infty} \frac{(HT_{\mathrm{I}} + \mu_n T_{\mathrm{w}}/\sinh \mu_n b)\nu_p}{(H + \mu_n \coth \mu_n b)(\mu_n^2 + \nu_p^2)}\right\}$$

and

$$\beta_{m,p} = \frac{4\nu_m}{ab(1 + \tanh \nu_p a)} \times \sum_{n=1}^{\infty} \frac{\mu_n^2}{(H + \mu_n \coth \mu_n b)(\mu_n^2 + \nu_p^2)(\mu_n^2 + \nu_m^2)}.$$

In the general case (i.e. $H \neq \infty$), the system of equation (6) can be solved for the f_p's only numerically. To do so the sum in equation (6) is first truncated to a finite number of terms, N. By varying the value of p from 1 to N in equation (6), a linear system of N equations with N unknowns (the coefficients f_p, $p = 1, 2, \ldots, N$) is obtained. This system can be solved

using the Gauss–Jordan elimination method. Once the coefficients f_p are found, they are substituted in equations (3) and (4) (in which the sums are also truncated to N terms) to obtain the temperature distributions $T_{\mathrm{I}}(x,y)$ and $T_{\mathrm{II}}(x,y)$, respectively. For the case of the slab-on-grade problem, it was found that $N = 15$ gives accurate estimations. Addition of other terms does not alter the results for T_{I} and T_{II} significantly (less than 0.01°C variation in soil temperature, for the cases treated in this paper).

Before proceeding further with the insulated slab-on-grade floor results, let us consider the limiting case of the non-insulated slab and perfect soil–slab contact (i.e. $H = \infty$).

2.2. *Prescribed slab-on-grade floor temperature*

When the slab is kept at a constant temperature T_i the temperature distribution inside the ground can be obtained from the above analysis by letting $H \to \infty$. In particular, the Fourier coefficients f_p can be determined in closed form, since $\beta_{m,p} = 0$ for all the values of m. It is found that

$$f_p = \frac{T_1 + T_0 \tanh \nu_p a}{\nu_p(1+\tanh \nu_p a)} - \frac{(-1)^n}{\nu_p} T_w. \tag{7}$$

Note the change in notation from T_1 to T_0. This is done on purpose to stress the fact that for a perfectly uninsulated floor, the slab temperature is uniform and equal to $T_i = T_0$. For an insulated floor, T_1 does not represent the temperature of the slab surface.

The substitution of f_p by its value and H by ∞, in equations (3) and (4) gives the temperatures in zones (I) and (II), respectively, as

$$T_{\mathrm{I}}(x,y) = T_1 - \frac{y}{b}(T_1 - T_w) + \frac{1}{\pi}\left\{\tan^{-1}\left[\frac{e^{\pi(x+a)/b}\sin \pi y/b}{1-e^{\pi(x+a)/b}\cos \pi y/b}\right] - \tan^{-1}\left[\frac{e^{\pi(x-a)/b}\sin \pi y/b}{1-e^{\pi(x-a)/b}\cos \pi y/b}\right]\right\}(T_0 - T_1) \tag{8}$$

and

$$T_{\mathrm{II}}(x,y) = T_0 - \frac{y}{b}(T_0 - T_w) + \frac{1}{\pi}\left\{\tan^{-1}\left[\frac{e^{-\pi(x+a)/b}\sin \pi y/b}{1-e^{-\pi(x+a)/b}\cos \pi y/b}\right] - \tan^{-1}\left[\frac{e^{-\pi(a-x)/b}\sin \pi y/b}{1-e^{-\pi(a-x)/b}\cos \pi y/b}\right]\right\}(T_1 - T_0). \tag{9}$$

Representative isotherms are shown for two cases in Fig. 2. In both cases, the half slab width a is equal to 3 m, while the water table depth is $b = 5$ m. Figure 3 shows the temperature variation with depth y along vertical surfaces.

A close look at Fig. 2 reveals that, in each of the two configurations, the isotherm $T = 22$°C meets perpendicularly, one of the three bounding surfaces: the slab, the soil surface, or the water table (i.e. the surface that is kept at the temperature $T = 22$°C, which is the medium of the three temperatures T_0, T_1, and T_w). The meeting point is what was called in ref. [10] the double point. The fact that, at this point, an isotherm is perpendicular to the bounding surface indicates that there is no heat flux at this location of the surface. In addition, the slab-on-grade floor configuration presents an axial symmetry around $x = 0$. Because of this symmetry it can be concluded from Fig. 2 that in most cases the surface which is kept at the medium of the three boundary surface temperatures T_{md} (i.e. $T_{md} = \mathrm{med}(T_0, T_1, T_w)$), has two double points. These two double points are symmetric to each other relative to the axis $x = 0$. Moreover, the two symmetric isotherms $T = T_{md}$ divide the ground into two zones, a *warm* zone and a *cold* zone. In the first zone, the temperature is always above T_{md}, and the heat flows in one direction: from the surface at the highest temperature to the surface at T_{md}. Conversely, in the second zone, the temperature never exceeds T_{md}, and the heat flow is always from the surface at T_{md} to the surface at the lowest temperature.

For example, consider the case of Fig. 2(a), in which the slab floor is kept at the medium temperature $T_{md} = T_0 = 22$°C. In this case the edge of the slab, part of the warm zone, gains heat from the soil surface (at 26°C). Meanwhile the center of the slab, losing heat to the water table surface (at 18°C), belongs to the cold zone of the ground.

Figure 4 shows the effect of the depth b on the heat flux distribution along the slab floor. The deeper the water table is, the narrower the central zone from which the slab loses heat. In other words, when b increases, the double points approach the center of the slab. This result agrees with Fig. 5 which shows the variation of the double point location as a function of water table depth b for different values of ΔT_0 ($\Delta T_0 = (T_0 - T_w)/(T_1 - T_0)$, $\Delta T_0 > 0$ implies the configuration $T_w < T_0 < T_1$).

2.3. *Insulated slab-on-grade floor results*

When the slab–soil contact is not thermally perfect or when the slab is insulated, the temperature along the floor surface is no longer constant. In fact, the insulation removes the temperature discontinuity at the floor edge, making the transition from the indoor temperature T_i to the soil surface temperature T_1 relatively smooth compared to the sudden transition noted in the case of an uninsulated slab. This transition becomes less abrupt as the insulation level increases. This fact is illustrated in Fig. 6; isotherms beneath a floor of half width $a = 3$ m, and above a water table of depth $b = 5$ m are shown. Different insulation configurations are presented.

The configuration of Fig. 6(c) ($H = 0.2$ m^{-1}) is particularly interesting. In this case all the isotherms are parallel to the soil surface, indicating a linear variation of the earth temperature with depth. This

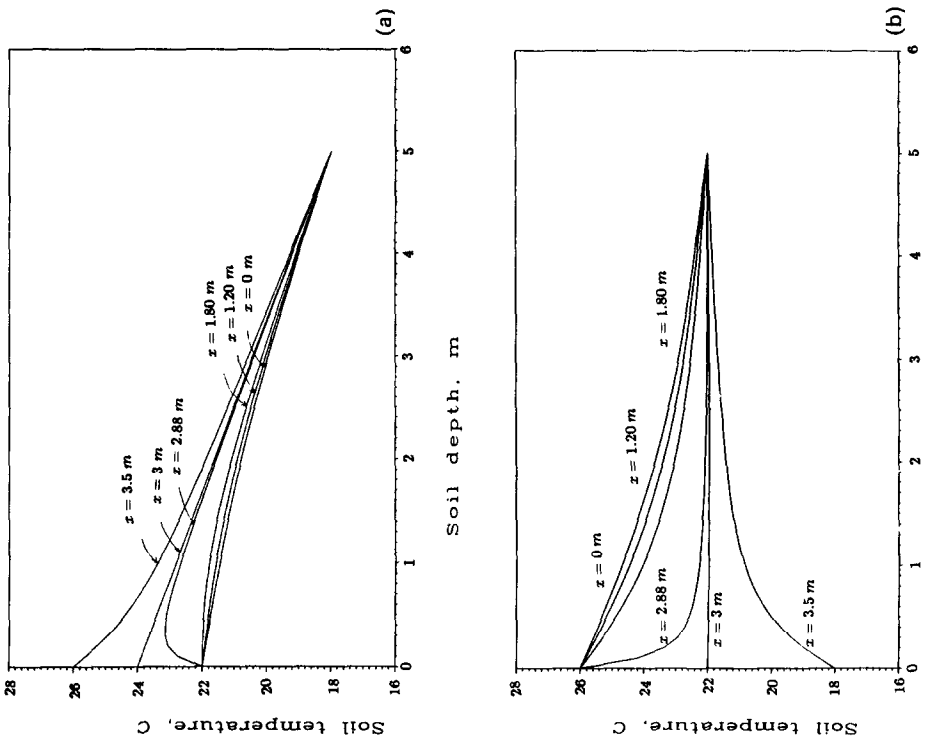

FIG. 3. Temperature variation with depth for various cross-sections in uninsulated slab-on-grade floor configuration with: (a) $T_0 = 22$°C, $T_1 = 26$°C, $T_w = 18$°C; (b) $T_0 = 26$°C, $T_1 = 18$°C, $T_w = 22$°C.

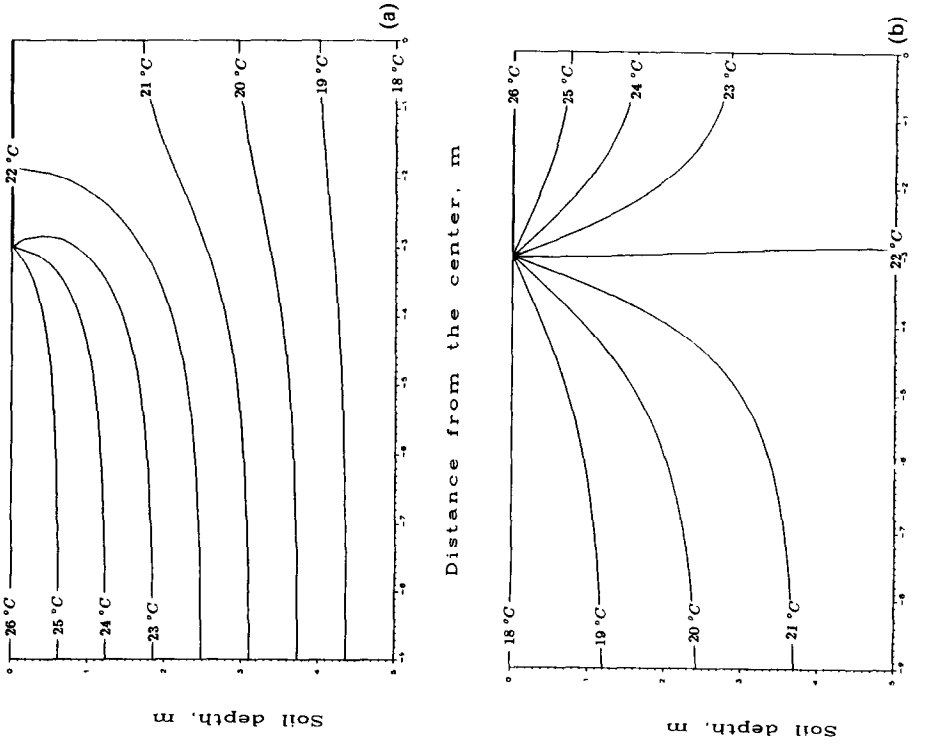

FIG. 2. Earth temperature isotherms beneath an uninsulated slab-on-grade floor with water table depth $b = 5$ m: (a) $T_0 = 22$ C, $T_1 = 26$°C, $T_w = 18$°C; (b) $T_0 = 26$°C, $T_1 = 18$°C, $T_w = 22$°C.

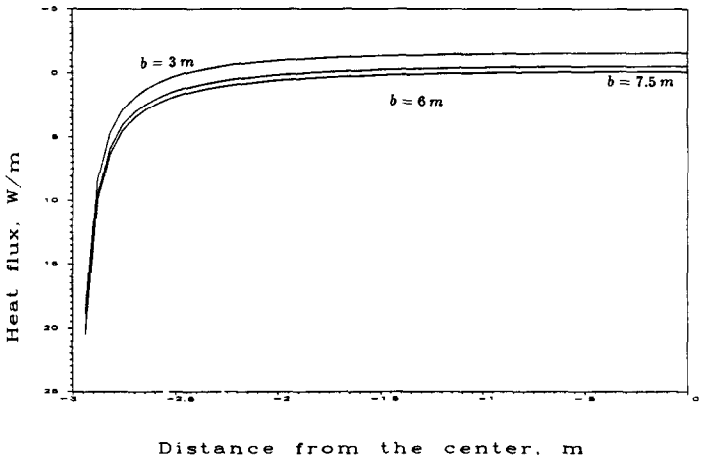

FIG. 4. Effect of water table depth on heat flux distribution along an uninsulated slab-on-grade floor.

particular result is general in a configuration where $T_w < T_1 < T_i$. In fact, the temperature inside the ground depends linearly on the depth y, when the parameter H is equal to a special value H_0 given by

$$H_0 = -\frac{1}{b}(1+\Delta T_0). \tag{10}$$

Note that $\Delta T_0 = (T_1 - T_w)/(T_1 - T_i) < -1$, in this case. The condition of equation (10) implies that the temperature along the slab surface is uniform and equal to the soil surface temperature T_1. In the configuration of Fig. 6(c), $\Delta T_0 = -2$, giving a value of $H_0 = 0.2\ m^{-1}$. In this case also note that the temperature of the slab is uniform and equal to $T_1 = 22°C$ while the room air temperature is 26°C.

From Fig. 6, one can see that the double point, which is initially beyond the slab edges, moves toward the slab edge, as the value of H decreases (e.g. as the result of an increase in the insulation). When $H = H_0$, the double point reaches the slab edge and stays there even after a further decrease in H. Equation (10) shows that an increase in the water depth b results in a decrease of the value of H_0, indicating that more insulation is needed to reach the case where heat is lost uniformly from the floor surface (case of Fig. 6(c)). In the limiting case when $b \to \infty$ (i.e. no water table), only perfect insulation leads to a uniform heat loss (of zero) from the floor.

In the case of Figs. 6(a) and (b), the floor loses heat to both the soil surface near the floor edges, and to the water surface from the central area. However, in the case of Figs. 6(c) and (d) a change in the heat flux pattern occurs. Here, the floor loses heat only to the water table.

Figure 7 shows the heat flux distribution along the floor surface, for the same temperature configuration of Fig. 6 (i.e. $T_w = 18°C$, $T_1 = 22°C$, $T_i = 26°C$). Two values of H are considered, 3.5 m^{-1} (Fig. 7(a)), and 0.5 m^{-1} (Fig. 7(b)). As one could expect, the heat loss is approximately constant near the slab center, but increases rapidly near the edges. In both Figs. 7(a) and (b) the heat loss at any point of the slab increases as the water depth b decreases. This increase is more noticeable at the center of the floor, since at this

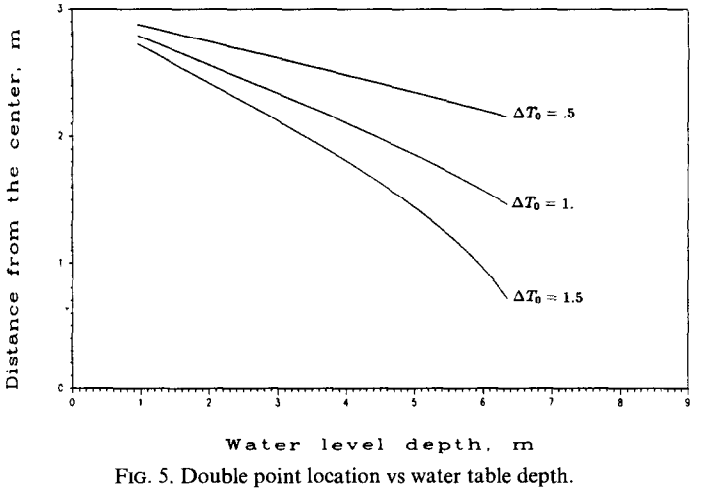

FIG. 5. Double point location vs water table depth.

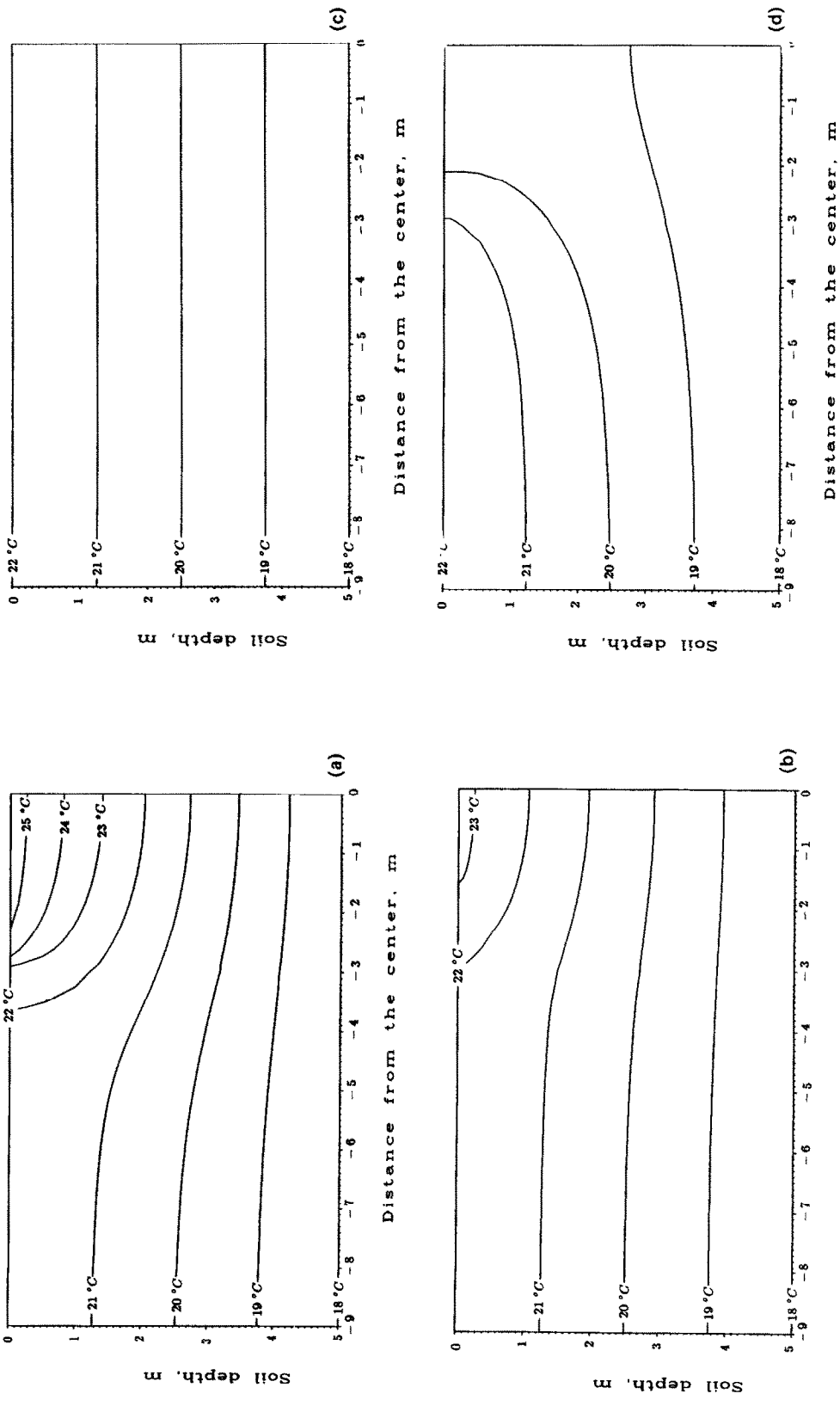

FIG. 6. Earth temperature isotherms beneath an insulated slab-on-grade floor with water table depth $b = 5$ m: (a) $H = 3.5$ m^{-1}; (b) $H = 0.5$ m^{-1}; (c) $H = 0.2$ m^{-1}; (d) $H = 0$ m^{-1}.

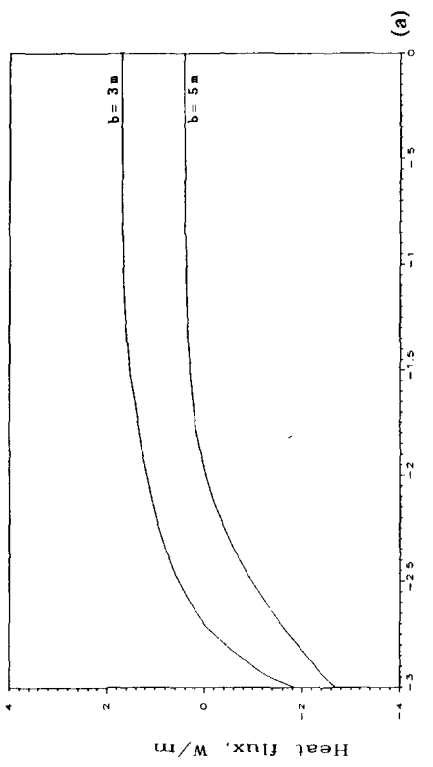

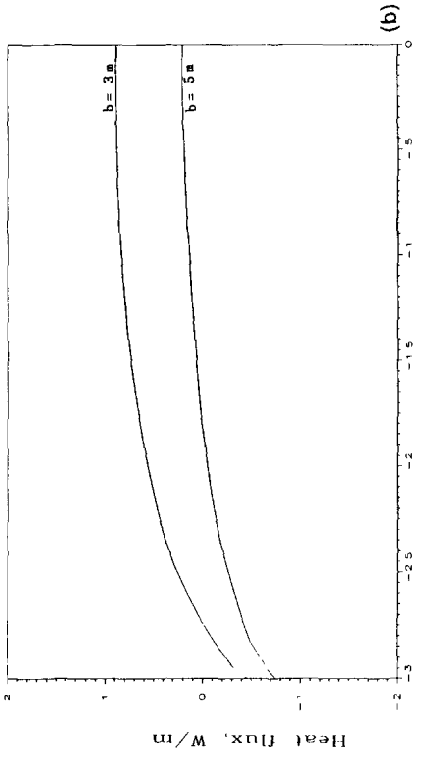

FIG. 8. Effect of water table depth on heat flux distribution along an insulated slab-on-grade floor with $T_i = 22$°C, $T_f = 26$ C, $T_w = 18$ C: (a) $H = 3.5$ m^{-1}; (b) $H = 0.5$ m^{-1}.

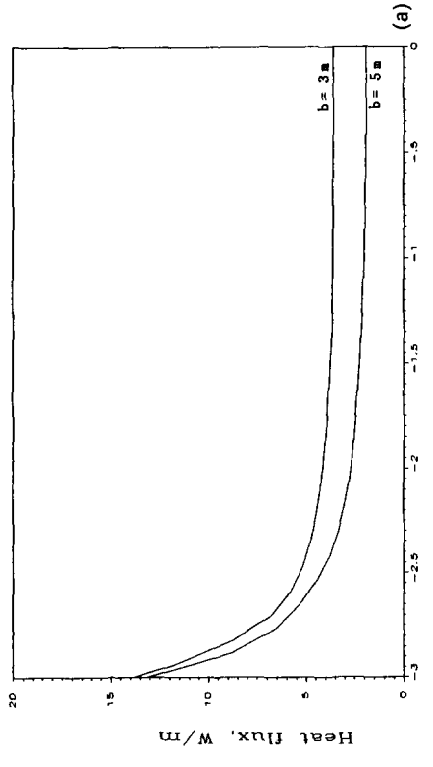

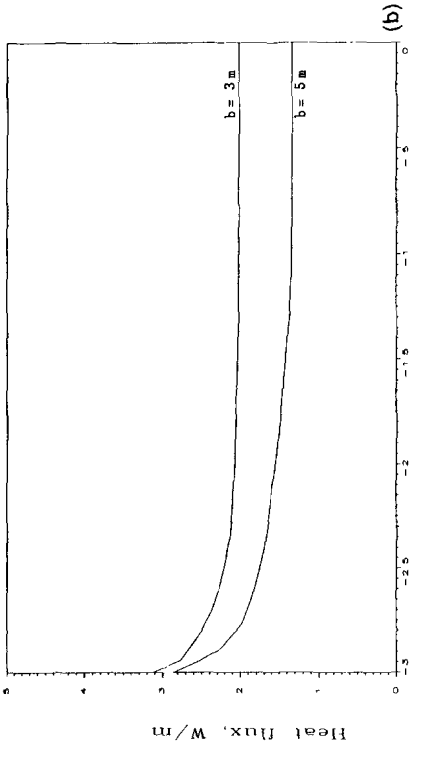

FIG. 7. Effect of water table depth on heat flux distribution along an insulated slab-on-grade floor with $T_i = 26$°C, $T_f = 22$°C, $T_w = 18$°C: (a) $H = 3.5$ m^{-1}; (b) $H = 0.5$ m^{-1}.

location, the heat loss is principally due to the presence of the water surface, which is at a lower temperature than the soil surface. Figure 8 gives the heat flux distribution along the floor surface, for a different temperature configuration ($T_w = 18°C$, $T_1 = 26°C$, $T_i = 22°C$). It is known in this case that the double point is located beneath the floor. The intersection point between the zero heat flux line and the heat flux distribution curve, marks the double point location. Both Figs. 8(a) ($H = 3.5\ m^{-1}$) and (b) ($H = 0.5\ m^{-1}$), show clearly that the floor surface is divided into two zones, one near the edges, gaining heat from the soil surface, and a second near the center, losing heat to the water surface. The area of the latter zone tends to decrease as the water depth increases.

3. INSULATED RECTANGULAR BASEMENT

For the basement problem a model different from that used previously will be introduced. Above, the temperature distribution was obtained along an infinite width of the ground (i.e. from $x = -\infty$ to ∞). The earth isotherms observed in the slab-edge and the slab-on-grade floor configurations indicated that the temperature varies linearly with depth, at locations far from the slab. For this reason, and especially for computational convenience, the basement problem is modelled as shown in Fig. 9. Along the bounding surfaces $x = \pm L$, the temperature is simply assumed to be a linear function of depth. In these conditions the temperature distribution $T(x, y)$, around the rectangular basement, is the solution of the following equation:

$$\frac{\partial^2 T}{\partial x^2} + \frac{\partial^2 T}{\partial y^2} = 0 \tag{11}$$

with

$$-\frac{\partial T}{\partial y} = H_f(T_i - T) \qquad \text{for } y = c \text{ and } |x| < a$$

$$-\frac{\partial T}{\partial x} = H_{wl}(T - T_i) \qquad \text{for } y < c \text{ and } |x| = a$$

$$T = T_1 \qquad \text{for } y = 0 \text{ and } |x| > a$$

$$T = T_1\left(1 - \frac{y}{b}\right) \qquad \text{for } |x| = L$$

$$T = 0 \qquad \text{for } y = b$$

where $H_f = h_f/k_s$ and $H_{wl} = h_{wl}/k_s$; h_f and h_{wl} are the values, respectively, of the air–insulation–floor–soil conductance and of the air–insulation–walls–soil conductance.

Note that in the formulation of equation (11) the water table temperature T_w was set to zero. This assumption is not restrictive since, for steady-state problems, the origin of temperature is arbitrary. A legitimate choice of this origin is T_w.

In order to solve the Laplace equation (i.e. equation (11)) by the ITPE technique, the ground is divided into five zones as indicated in Fig. 9. Since the basement configuration has an axial symmetry around $x = 0$, the determination of the temperature variation in zones (I), (II), and (III) will be sufficient. Furthermore, the temperature profiles at the surfaces $x = -a$ and $y = c$ are functions of y and x, respectively

$$T(-a, y) = f(y), \quad c < y < b$$

and

$$T(x, c) = g(x), \quad -L < x < -a.$$

Using the separation of variables technique, the solution in zone (I) is

$$T_I(x, y) = \frac{2}{(b-c)} \sum_{n=1}^{\infty} f_n \sin \nu_n(y-c) \frac{\cosh \nu_n x}{\cosh \nu_n a} - \frac{2}{a} \sum_{n=1}^{\infty} A_n \cos \mu_n x \frac{\sinh \mu_n(b-y)}{\sinh \mu_n(b-c)}. \tag{12}$$

In zone (III), the solution is given by

$$T_{III}(x, y) = \frac{2}{(L-a)} \sum_{n=1}^{\infty} g_n \sin \chi_n(x+a) \frac{\sinh \chi_n(b-y)}{\sinh \chi_n(b-c)} + \frac{2}{(b-c)} \sum_{n=1}^{\infty} f_n \sin \nu_n(y-c) \frac{\sinh \nu_n(x+L)}{\sinh \nu_n(L-a)} + \frac{2}{(b-c)} T_1 \sum_{n=1}^{\infty} \frac{(b-c)/b}{\nu_n} \sin \nu_n(y-c) \frac{\sinh \nu_n(x+a)}{\sinh \nu_n(a-L)}. \tag{13}$$

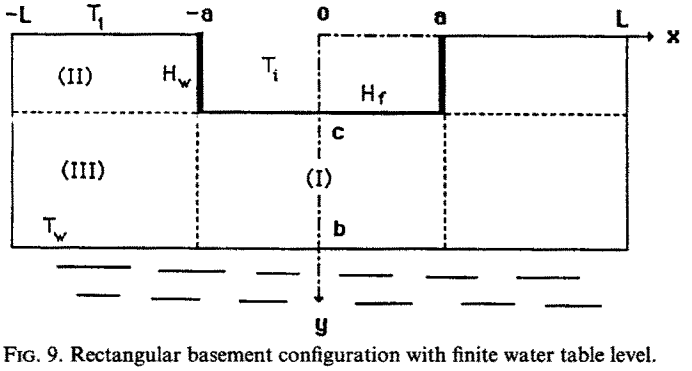

FIG. 9. Rectangular basement configuration with finite water table level.

The expression for the temperature in zone (II) takes a more complex form

$$T_{II} = \frac{2}{(L-a)} T_1 \sum_{n=1}^{\infty} \frac{[(-1)^n - 1]}{\chi_n} \sin \chi_n (x+a) \times \frac{\sinh \chi_n (c-y)}{\sinh \chi_n c} + \frac{2}{(L-a)} \sum_{n=1}^{\infty} g_n \sin \chi_n \frac{\sinh \chi_n y}{\sinh \chi_n c} + \frac{2}{c} T_1 \sum_{n=1}^{\infty} \frac{[1-(-1)^n (b-c)/b]}{\zeta_n} \sin \zeta_n y \frac{\sinh \zeta_n (x+a)}{\sinh \zeta_n (a-L)} + \frac{2}{c} \sum_{n=1}^{\infty} B_n \sin \zeta_n y \frac{\sinh \zeta_n (x+L)}{\sinh \zeta_n (L-a)} \quad (14)$$

where

$$\nu_n = \frac{n\pi}{(b-c)}; \quad \chi_n = \frac{n\pi}{(L-a)}$$

$$\zeta_n = \frac{n\pi}{c}; \quad \mu_n = \frac{(2n-1)\pi}{2a}$$

$$f_n = \int_c^b f(y) \sin \nu_n (y-c)\, dy$$

$$g_n = \int_{-L}^{-a} g(x) \sin \chi_n (x+a)\, dx$$

$$A_n = \frac{(-1)^n H_f T_i / \mu_n}{H_f + \mu_n \coth \mu_n (b-c)} + \frac{2(-1)^n}{(b-c)} \sum_{m=1}^{\infty} \frac{f_m \nu_m \mu_n / (\nu_m^2 + \mu_n^2)}{H_f + \mu_n \coth \mu_n (b-c)}$$

$$B_n = \frac{[1-(-1)^n] H_{w1} T_i / \zeta_n - [1-(-1)^n (b-c)/b] T_1 / \sinh \zeta_n (a-L)}{H_{w1} + \zeta_n \coth \zeta_n (L-a)} - \frac{2}{(L-a)} \sum_{m=1}^{\infty} \frac{\{\chi_m \zeta_n g_m - [1-(-1)^n] \zeta_n T_1\} / (\chi_m^2 + \zeta_n^2)}{H_{w1} + \zeta_n \coth \zeta_n (L-a)}$$

The Fourier coefficients f_n and g_n can be determined from the required continuity of the heat flux along the surfaces $x = -a$ and $y = c$. First, for $x = -a$, flux continuity states that

$$\left.\frac{\partial T_I}{\partial x}\right|_{x=-a} = \left.\frac{\partial T_{III}}{\partial x}\right|_{x=-a}. \quad (15)$$

After a computation procedure similar to that followed in the slab-on-grade section, the condition given by equation (15) leads to

$$\nu_p [\tanh \nu_p a + \coth \nu_p (L-a)] f_p = \gamma_p + \sum_{n=1}^{\infty} \alpha_{n,p} f_n + \sum_{n=1}^{\infty} \beta_{n,p} g_n \quad (16)$$

with

$$\gamma_p = \frac{2}{a} \sum_{n=1}^{\infty} \frac{H_f \nu_p T_i}{[H_f + \mu_n \coth \mu_n (b-c)](\nu_p^2 + \mu_n^2)} + \frac{(b-c) T_1}{b \sinh \nu_p (L-a)}$$

$$\beta_{n,p} = -\frac{2}{(L-a)} \frac{\chi_n \nu_p}{\chi_n^2 + \nu_p^2}$$

$$\alpha_{n,p} = \frac{4}{a(b-c)} \times \sum_{m=0}^{\infty} \frac{\nu_n \nu_p \mu_m^2}{[H_f + \mu_m \coth \mu_m (b-c)](\nu_p^2 + \mu_m^2)(\nu_n^2 + \mu_m^2)}.$$

The condition of the heat flux continuity at the surface $y = c$ is expressed by

$$\left.\frac{\partial T_{II}}{\partial y}\right|_{y=c} = \left.\frac{\partial T_{III}}{\partial y}\right|_{y=c}. \quad (17)$$

This condition yields a system of equations of the form of

$$\chi_p [\coth \chi_p c + \coth \chi_p (b-c)] g_p = \gamma'_p + \sum_{m=1}^{\infty} \alpha'_{m,p} g_m + \sum_{m=1}^{\infty} \beta'_{m,p} f_m \quad (18)$$

where

$$\gamma'_p = -[1-(-1)^p] \frac{T_1}{\sinh \chi_p c} + (1-c/b)(-1)^p T_1 \times \left[\coth \chi_p (b-c) + \frac{1}{\chi_p (b-c)}\right] - (-1)^p T_1 \left(\frac{c}{b} \coth \chi_p c - \tanh \frac{\chi_p c}{2} - \frac{1}{\chi_p b}\right) - \frac{2}{c} T_1 \sum_{n=1}^{\infty} \frac{[1-(-1)^n] \chi_p H_{w1}}{[H_{w1} + \zeta_n \coth \zeta_n (L-a)](\chi_p^2 + \zeta_n^2)} + \frac{2}{c} T_1 \left(\sum_{n=1}^{\infty} \frac{\chi_p \zeta_n [1-(-1)^n (1-c/b)] / \sinh \zeta_n (L-a)}{[H_{w1} + \zeta_n \coth \zeta_n (L-a)](\zeta_n^2 + \chi_p^2)} + \sum_{n=1}^{\infty} \frac{\zeta_n [1-(-1)^n] \{\coth (\zeta_n (L-a)) - 1/[\zeta_n (L-a)]\}}{[H_{w1} + \zeta_n \coth \zeta_n (L-a)](\zeta_n^2 + \chi_p^2)} \right)$$

$$\alpha'_{m,p} = -\frac{4}{c(L-a)} \times \sum_{n=1}^{\infty} \frac{(-1)^n \zeta_n^2 \chi_p \chi_m}{[H_{w1} + \zeta_n \coth \zeta_n (L-a)](\zeta_n^2 + \chi_p^2)(\zeta_n^2 + \chi_m^2)}$$

$$\beta'_{m,p} = -\frac{2}{(b-c)} \frac{\nu_m \chi_p}{\nu_m^2 + \chi_p^2}.$$

The procedure developed for determining the slab-on-grade solution can be repeated, with some appropriate adjustments. To find the temperature distribution around a rectangular basement for specific boundary temperatures, water depth, and insulation configuration, two steps are needed.

(1) The Fourier coefficients f_p and g_p are determined by truncating the sums in equation (16), and in equation (18) to N terms. By doing so, a system of $2N$ equations with $2N$ unknowns ($f_1, f_2, \ldots, f_N$ and $g_1, g_2, \ldots, g_N$) is obtained. This system can be easily solved using standard methods (e.g. Gauss–Jordan elimination). In all basement configurations treated in this section, $N = 20$ was needed to reach an accuracy of 0.01°C for the soil temperature.

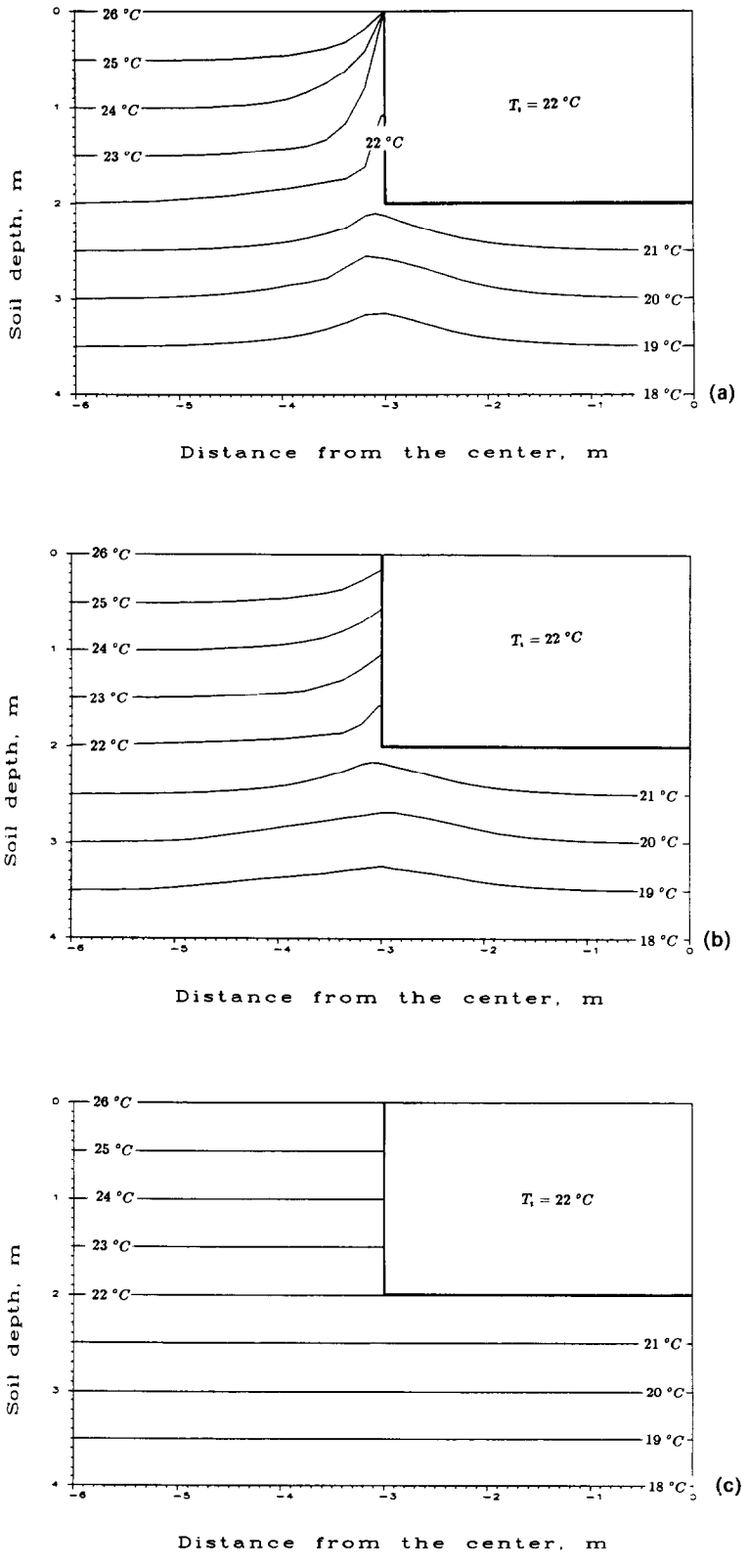

FIG. 10. Earth temperature isotherms around a basement with water table depth $b = 4$ m, $T_i = 22°C$, $T_1 = 26°C$, $T_w = 18°C$, $H_f = \infty$: (a) $H_{wl} = \infty$; (b) $H_{wl} = 0.5\ m^{-1}$; (c) $H_{wl} = 0\ m^{-1}$.

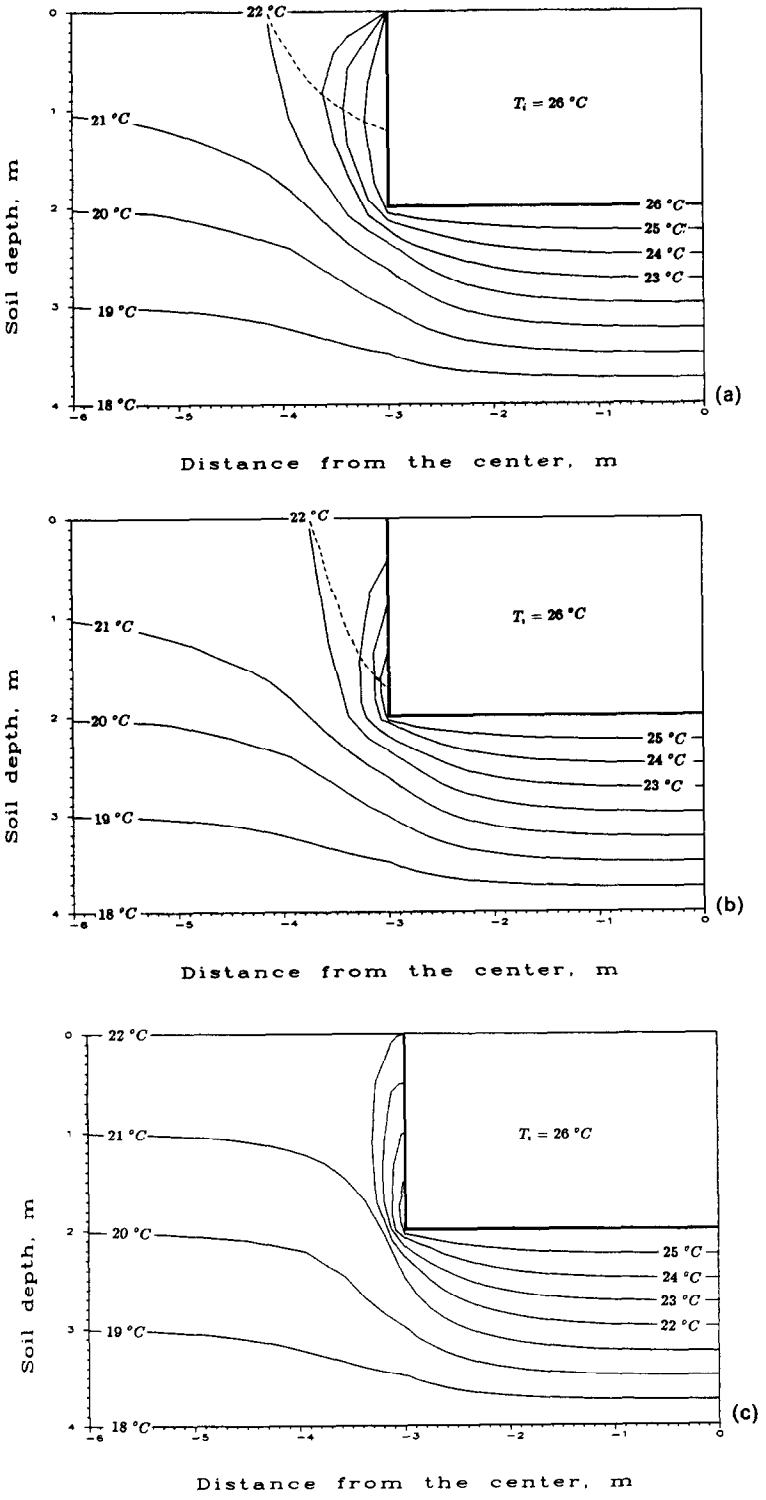

FIG. 11. Earth temperature isotherms around a basement with water table depth $b = 4$ m, $T_i = 26°C$, $T_1 = 22°C$, $T_w = 18°C$, $H_f = \infty$: (a) $H_{wl} = \infty$; (b) $H_{wl} = 0.5\ m^{-1}$; (c) $H_{wl} = 0\ m^{-1}$.

(2) The temperatures inside zones (I), (II), and (III) are found by substitution of the values of the Fourier coefficients f_p and g_p into equations (12)–(14), respectively.

Figure 10 illustrates the results of these two steps for a basement of half width $a = 3$ m, and a depth $c = 2$ m. The air inside the basement is at a temperature $T_i = 22°C$ while the soil surface temperature $T_1 = 26°C$. A water table below the basement floor at a depth $b = 4$ m, is kept at $T_w = 18°C$. Three wall insulation configurations are treated $H_{wl} = \infty$ in Fig. 10(a), $H_{wl} = 0.5\ m^{-1}$ in Fig. 10(b), and $H_{wl} = 0$ in Fig. 10(c). In all these configurations, the basement floor is assumed to be perfectly uninsulated (i.e. $H_f = \infty$). At the point of connection between the soil surface and the basement wall, many isotherms meet (Fig. 10(a)). This indicates that, at this point, the heat flux is relatively large. However, when H_{wl} decreases, the isotherms separate and the heat flux decreases (Figs. 10(b) and (c)). At the same time, the double point, initially located near the center of the wall surface, starts to move to the bottom of the wall. Again, it can be seen that this double point divides the wall into two regions. The upper part receives heat from the soil surface while the lower part loses heat to the water surface. Therefore, as H_{wl} decreases (by increasing insulation), the wall benefits more from the soil surface than the water surface from the wall, at least as far as heat exchange is concerned.

Moreover, and always referring to Fig. 10, it is clear that when the wall is perfectly insulated ($H_{wl} = 0$), the ground temperature becomes a simple linear function of the depth y. In general, this situation occurs in the case where $-1 < \Delta T_0 = (T_i - T_w)/(T_1 - T_i) < 0$ (e.g. $T_w < T_i < T_1$), with the conditions: $H_{wl} = 0$, $H_f = \infty$, and

$$c = b(1 + \Delta T_0)^{-1}. \tag{19}$$

In the case of Fig. 10(c), since $\Delta T_0 = 1$, $b = 4$ m, and $c = 2$ m, the condition of equation (19) is indeed met and the profile with depth is linear.

Figure 11 shows some ground isotherms around a rectangular basement, similar to that in Fig. 10, but with $T_1 = 22°C$, $T_i = 26°C$, and $T_w = 18°C$. The double point on the soil surface first moves along the basement wall toward the basement floor as the wall insulation increases (i.e. H_{wl} decreases). This means that the soil surface receives progressively less heat from the basement wall. However, the area of the basement wall, from which this heat is lost to the soil surface, becomes larger. In fact, the dashed line in Fig. 11 marks a limiting heat flow line. Above this line, heat flows solely towards the soil surface. In the case of Fig. 11(c), this line coincides with the wall surface, since heat cannot be lost (perfect wall insulation, $H_{wl} = 0$).

4. CONCLUSIONS

A semi-analytical procedure has been developed to solve some complicated heat conduction problems. This procedure has been used to carry out a detailed investigation of heat transfer from the ground to adjacent buildings with slab floors and basements. The importance of envelope insulation, water table temperature and geometric dimensions on the heat flow mechanism within soil is evaluated. Examination of soil temperature profiles in the two earth-contact structures treated in this paper shows that heat near the center of floors flows mostly in one dimension but near the walls and the floor it has a definite two-dimensional nature. Two other important results can be mentioned.

(1) The double point concept was established when a water table is present below a building foundation. The location of the double point on a given surface marks a change in the heat flow direction. On one side of the double point, the surface loses heat but on the other side it gains heat.

(2) Particular insulation values and configurations exist for which soil temperature is simply a linear function of depth, indicating that the soil is thermally undisturbed even though a building is present.

Acknowledgement—A portion of this work was supported by a Grant-in-Aid awarded to Moncef Krarti by the American Society of Heating Refrigerating and Air Conditioning Engineers. This support is gratefully acknowledged.

REFERENCES

1. M. Krarti, Application of a new approximate analytical method to ground coupling problems, M.S. Thesis, University of Colorado, Boulder, Colorado (1985).
2. M. Krarti, D. E. Claridge and J. F. Kreider, Interzone temperature profile estimation—slab-on-grade heat transfer results. In *Heat Transfer in Buildings and Structures*, HTD-41, pp. 11–20. ASME, New York (1985).
3. M. Krarti, D. E. Claridge and J. F. Kreider, Interzone temperature profile estimation—below grade basement heat transfer results. In *Heat Transfer in Buildings and Structures*, HTD-41, pp. 21–29. ASME, New York (1985).
4. J. Shelton, Underground storage of heat in solar heating systems, *Solar Energy* **17**, 137–143 (1975).
5. G. G. Boileau and J. K. Latta, Calculation of basement heat losses, Technical Paper No. 292, Division of Building Research, NRC Canada, Ottawa (1968).
6. *ASHRAE Handbook: 1981 Fundamentals*. American Society of Heating, Refrigerating and Air Conditioning Engineers, Atlanta, Georgia (1981).
7. L. S. Shen and J. W. Ramsey, A simplified thermal analysis of earth-sheltered buildings using a Fourier-series boundary method, *ASHARE Trans.* **89**(1B), 438–448 (1983).
8. J. Claesson and B. Eftring, Optimal thermal insulation and ground heat losses, Lund Institute of Technology, Department of Mathematical Physics, Lund, Sweden (August 1979).
9. D. E. Claridge, Design methods for earth-contact heat transfer. In *Progress in Solar Energy* (Edited by K. Boer). American Solar Energy Society, Boulder, Colorado (1986).
10. M. Krarti, D. E. Claridge and J. F. Kreider, The Schwartz–Christoffel transformation applied to ground-coupling problems, presented at the 1988 ASME Solar Energy Division Conference (April 1988).

APPLICATION DE LA TECHNIQUE ITPE A DES PROBLEMES PERMANENTS DE COUPLAGE AU SOL

Résumé—Une nouvelle procédure appelée Estimation du Profil de Température Interzone (ITPE) est présentée et appliquée à la détermination de la distribution bidimensionnelle permanente de température dans le sol autour d'un bâtiment. Les solutions des équations de convection sont obtenues pour deux géométries courantes de couplage au sol: étages sur une semelle et fondations rectangulaires. Une nappe d'eau à température constante est supposée exister à une profondeur donnée au dessous de la surface du sol. Les solutions présentées sont les premières, pour ces géométries, qui soient capables de considérer les effets à la fois de l'isolation et de la présence d'une nappe d'eau sur la conduction de chaleur avec des géométries.

DIE ANWENDUNG DER ITPE-TECHNIK BEI STATIONÄREN ERDBODEN-MODELLEN

Zusammenfassung—Eine neue analytische Vorgehensweise namens ITPE (Interzone Temperature Profile Estimation) wird vorgestellt und verwendet, um die zwei-dimensionale stationäre Temperaturverteilung innerhalb des Erdbodens um ein Gebäude zu bestimmen. Die Wärmeleitungsgleichungen für zwei gebräuchliche Erdbodengeometrien werden gelöst: für einen oberflächengleichen Gebäudeboden und für einen rechteckigen Keller. In einer gegebenen Tiefe unterhalb der Erdbodenoberfläche wird die Existenz einer wasserführenden Schicht von konstanter Temperatur angenommen. Die gezeigten Lösungen sind die ersten analytischen für diese Geometrien, die in der Lage sind, die Auswirkungen sowohl der Wärmedämmung, als auch das Vorhandensein einer wasserführenden Schicht auf den Wärmestrom bei den genannten geometrischen Anordnungen zu berücksichtigen.

ИСПОЛЬЗОВАНИЕ МЕТОДА ОПРЕДЕЛЕНИЯ МЕЖЗОНАЛЬНОГО ПРОФИЛЯ ТЕМПЕРАТУР ДЛЯ РЕШЕНИЯ СТАЦИОНАРНЫХ ЗАДАЧ ТЕПЛООБМЕНА ЗДАНИЯ С ЗЕМЛЕЙ

Аннотация—Предложен новый аналитический метод под названием "определение межзонального профиля температур (ОМПТ)", который используется для нахождения двумерного стационарного распределения температуры внутри земляного массива вокруг здания. Получены решения уравнений теплопроводности для двух широко распространенных геометрий: настилов из плит на уровне земли и прямоугольных подвалов. Предполагается залегание грунтовых вод постоянной температуры на определенной глубине ниже уровня земли. Для таких геометрий впервые представлены аналитические решения, учитывающие влияние как изоляции, так и грунтовых вод на потери тепла такими объектами.